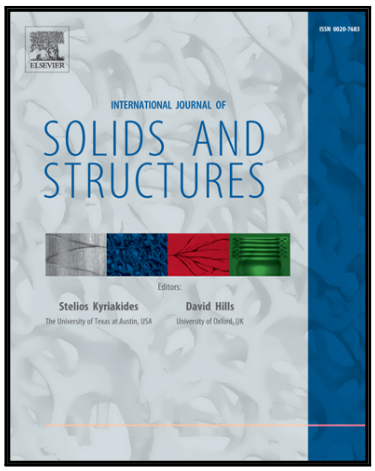

Explicit effective elasticity tensors of two-phase periodic composites with spherical or ellipsoidal inclusions

Quy-Dong To, Guy Bonnet, Duc-Hieu Hoang

PII: S0020-7683(16)30075-0
DOI: 10.1016/j.ijsolstr.2016.05.005
Reference: SAS 9164

To appear in: *International Journal of Solids and Structures*

Received date: 24 October 2015
Revised date: 2 May 2016
Accepted date: 6 May 2016

Please cite this article as: Quy-Dong To, Guy Bonnet, Duc-Hieu Hoang, Explicit effective elasticity tensors of two-phase periodic composites with spherical or ellipsoidal inclusions, *International Journal of Solids and Structures* (2016), doi: 10.1016/j.ijsolstr.2016.05.005

Explicit effective elasticity tensors of two-phase periodic composites with spherical or ellipsoidal inclusions

Quy-Dong To[a,b,*], Guy Bonnet[a], Duc-Hieu Hoang[a]

[a] *Université Paris-Est, Laboratoire Modelisation et Simulation Multi Echelle, UMR 8208 CNRS, 5 Boulevard Descartes, 77454 Marne-la-Vallée Cedex 2, France*
[b] *Duy Tan University - Institute of Research & Development, K7/25 Quang Trung, Danang, Vietnam*

Abstract

The effective elasticity tensors of two-phase composites are estimated by solving the localization problem in the wave-vector domain for the case of non overlapping spherical or ellipsoidal inclusions. With previous works showing that the effective properties can be computed from lattice sums, we propose a method to compute the sums analytically and obtain the explicit expressions for the effective tensors. In the case of different periodic cells leading to cubic or orthotropic elasticity tensors, the effective elasticity tensors are obtained in closed forms that are in good agreement with the exact solutions for a large range of physical parameters. In the random distribution cases, the statistical connection of the effective tensor to the structure factor is shown and a closed-form expression is obtained in the infinite volume limit.

Keywords: Closed-form expression; Fourier transform; effective elasticity tensors; non overlapping spherical inclusions; ellipsoidal inclusions; periodic problem; random distribution; orthorhombic lattice; structure factor; form factor

*Email: quy-dong.to@u-pem.fr

1. Introduction

One objective of micromechanics is to model the overall behavior of composites by studying physical problems at the scale of heterogeneities, followed by averaging the physical quantities on volumes of interest. The usual homogenization procedure is to construct a representative volume element (RVE) containing the distribution of different constituting phases and then to use continuum mechanics to analyze the localization problem. For elastic periodic media, it was shown that the effective elasticity tensor is rigorously defined from the average stress/strain linear relation (Sanchez-Palencia, 1974, 1980) obtained by studying only a unit cell.

Most closed-form estimations of the effective elasticity tensor are based on simplifications of RVE containing assemblages of coated spheres or ellipsoids (Eshelby, 1957; Christensen and Lo, 1979; Benveniste and Milton, 2003; Tsukrov and Kachanov, 2000). For periodic problems, the solutions are usually obtained from numerical methods such as the finite element method (FEM), boundary element method (BEM) and fast Fourier transform (FFT) (Kaminski, 1999, 2005; Liu et al., 2005; Michel et al., 1999; Eyre and Milton, 1999; Monchiet and Bonnet, 2012). Generally, it is more difficult to apply analytical techniques to periodic microstructures due to the special boundary conditions and the geometry of the unit cell. The most sophisticated complete semi-analytical methods use an expansion of the solution on the basis of periodic functions and expand the basis functions on spherical harmonics or spheroidal functions (Nunan and Keller, 1984; Sangani and Lu, 1987; Kushch, 1997, 2013), whereas estimates can be obtained by perturbation methods (Cohen, 2004).

In this paper, we use the Nemat-Nasser-Iwakuma-Hejazi (NIH) approximation (Nemat-Nasser et al., 1982) to treat the specific case of two-phase periodic composites with spherical or ellipsoidal inclusions. This method has

the same level of approximation as provided by the Clausius-Mossotti (CM) assumption, that is, it provides good estimates for a large range of inclusion concentrations. It takes into account the distribution of inclusions, but it is not more accurate for very large concentrations of inclusions. In this context, it rests on Fourier expansion and is very versatile, thus accounting for the interaction between inclusions or cracks of different kinds: such as ellipsoids, and cuboids. Further, it can address a fully anisotropic behavior. This method is much easier to use than fully numerical methods. Nevertheless, it necessitates the computation of lattice sums, which requires obviously a minimum of numerical calculations: storing a large number of Fourier components, checking the convergence of the lattice sums, etc. In some cases, like for some cubic cases, alternative methods provided, under similar assumptions, simple expressions of the effective elasticity tensors (Cohen, 2004). For further applications, the computation of lattice sums for further applications has been to interpolate can also be avoided by interpolating some results coming from the NIH method, like for fiber composites (Luciano and Barbero, 1994). The main contribution of our work is also to avoid the computation of the lattice sums, but by estimating these sums analytically in more general periodic cells containing spheres or ellipsoids. By considering such different arrangements inside the unit cell (e.g., simple orthorhombic (SO), body-centered orthorhombic (BCO), and face-centered orthorhombic (FCO)), we derive explicit closed-form expressions of the effective elasticity tensors.

The next part of this work deals with the random distribution case. As an extension of our previous work on conduction phenomena (To et al., 2013; To and Bonnet, 2015), we establish the statistical connections between the effective tensor and local arrangement factors such as the form factor $\mathcal{P}(\boldsymbol{\xi})$, the structure factor $S(\boldsymbol{\xi})$, and the scattering intensity $\mathcal{I}(\boldsymbol{\xi})$ used in the scattering theory (Hunter and White, 2001; Bohren and Huffman, 1998) and more

generally in solid-state physics (Rössler, 2009). These factors provide useful insight into the local structure of the particles, and it is worth noting that they can be obtained experimentally. Finally, a closed-form solution is also obtained in this case.

The present paper is composed of five sections. After the Introduction, Section 2 is dedicated to the homogenization theory of periodic media using the integral equation approach and NIH estimation. In Section 3, closed-form solutions for elasticity tensors related to different arrangements of spherical or ellipsoidal inclusions are derived. Section 4 deals with the random cases; some numerical applications and comparisons with different solutions of the literature are reported in Section 5 and finally, the summary and remarks are presented in Section 6.

The usual notations of tensor algebra are adopted throughout the paper. For example, tensors are in bold characters, tensor products are denoted by "$\otimes$" (tensor products) and "$.,:$" (inner products). The Einstein summation convention is used for repeated indices.

2. Homogenization of elastic periodic composites

First, the governing integral equations of the homogenization problem are derived along classical means (Christensen, 1979; Milton, 2002), however with more attention given to the periodic case and the use of Fourier transforms. Next, the estimation of effective elasticity tensors based on the integral equations (Nemat-Nasser et al., 1982) is introduced.

2.1. Governing integral equations

We consider an infinite elastic composite the fourth-order elasticity tensor $\mathbb{C}$ of which is a periodic function of the local coordinates $\mathbf{x}(x_1, x_2, x_3)$ with

periods a_1, a_2, a_3:

$$\mathbb{C}(x_1, x_2, x_3) = \mathbb{C}(x_1 + n_1 a_1, x_2 + n_2 a_2, x_3 + n_3 a_3), \quad \forall n_1, n_2, n_3 \in \mathbb{Z} \quad (1)$$

The homogenization procedure of the periodic material was rigourously established from the asymptotic development of the involved quantities, stress $\boldsymbol{\sigma}$, strain $\boldsymbol{\epsilon}$, and displacement $\mathbf{u}$ in terms of the scaling parameter ε (Sanchez-Palencia, 1974, 1980). Matching the powers of ε in the elasticity equations yields different relations between the quantities, including the definition of the effective elasticity tensor $\mathbb{C}^e$. To summarize, the following periodic boundary value problem in a unit cell V:

$$\begin{aligned}
&\boldsymbol{\sigma}(\mathbf{x}) = \mathbb{C}(\mathbf{x}) : \boldsymbol{\epsilon}(\mathbf{x}) \quad \forall \mathbf{x} \in V \\
&\boldsymbol{\epsilon}(\mathbf{x}) = \frac{1}{2}(\nabla \mathbf{u}(\mathbf{x}) + \nabla^T \mathbf{u}(\mathbf{x})), \quad \forall \mathbf{x} \in V \\
&\nabla \cdot \boldsymbol{\sigma}(\mathbf{x}) = 0, \quad \forall \mathbf{x} \in V \\
&\mathbf{u}(\mathbf{x}) - \mathbf{E}.\mathbf{x} \quad \text{periodic}, \\
&\boldsymbol{\sigma}(\mathbf{x}).\mathbf{n} \quad \text{antiperiodic}
\end{aligned} \quad (2)$$

must be solved, allowing finally the computation of the effective elasticity tensor $\mathbb{C}^e$ from the relation between macroscopic strain $\mathbf{E}$ and stress $\boldsymbol{\Sigma}$:

$$\boldsymbol{\Sigma} = \mathbb{C}^e : \mathbf{E}, \quad \boldsymbol{\Sigma} = \langle \boldsymbol{\sigma} \rangle_V, \quad \mathbf{E} = \langle \boldsymbol{\epsilon} \rangle_V. \quad (3)$$

Here, we adopt the notation $\langle \rangle_V$ to refer to the average over volume V of the quantity inside the brackets, for example,

$$\langle \boldsymbol{\phi} \rangle_V = \frac{1}{V} \int \boldsymbol{\phi} dV. \quad (4)$$

Due to the periodicity of the problem, it is useful to express the periodic quantities in the form of Fourier series and apply Fourier analysis to the elasticity equations (2). For example, if $\boldsymbol{\phi}$ is a periodic function of x_1, x_2, x_3,

it can be expressed as a Fourier series:

$$\boldsymbol{\phi}(\mathbf{x}) = \sum_{\boldsymbol{\xi}\neq 0} \boldsymbol{\phi}(\boldsymbol{\xi}) e^{i\boldsymbol{\xi}.\mathbf{x}}, \quad \boldsymbol{\phi}(\boldsymbol{\xi}) = \left\langle \boldsymbol{\phi}(\mathbf{x}) e^{-i\boldsymbol{\xi}.\mathbf{x}} \right\rangle_V, \tag{5}$$

where $\boldsymbol{\phi}$ can be stress $\boldsymbol{\sigma}$, strain $\boldsymbol{\epsilon}$, elasticity tensor $\mathbb{C}$, etc. For the sake of simplicity, we differentiate quantities in Fourier space and in real space by adding the variable after the same symbol: $\boldsymbol{\phi}(\boldsymbol{\xi})$ is the Fourier transform of the real function $\boldsymbol{\phi}(\mathbf{x})$ defined by $(5)_2$. We note that the infinite sum in $(5)_1$ involves all discrete wave vectors $\boldsymbol{\xi}$ with components ξ_1, ξ_2 and ξ_3 satisfying

$$\xi_i = \frac{2\pi n_i}{a_i}, \quad i = 1, 2, 3, \quad n_1, n_2, n_3 \in \mathbb{Z}. \tag{6}$$

The periodic boundary value problem (2) can be solved by an integral equation approach. By introducing a constant reference elasticity tensor $\mathbb{C}^0$ and polarization tensor $\boldsymbol{\sigma}^*$ (or eigenstress tensor) defined by

$$\boldsymbol{\sigma}(\mathbf{x}) = \mathbb{C}^0 : \boldsymbol{\epsilon}(\mathbf{x}) + \boldsymbol{\sigma}^*(\mathbf{x}), \tag{7}$$

it can be shown that $\boldsymbol{\epsilon}, \boldsymbol{\sigma}$ can be determined via the expressions

$$\boldsymbol{\epsilon}(\boldsymbol{\xi}) = -\boldsymbol{\Gamma}^0(\boldsymbol{\xi}) : \boldsymbol{\sigma}^*(\boldsymbol{\xi}). \tag{8}$$

In (8), $\boldsymbol{\Gamma}^0(\boldsymbol{\xi})$ is the Green operator for strain in Fourier space. When the reference material is isotropic with Lamé constants λ_0 and μ_0, for example,

$$C^0_{ijkl} = \lambda_0 \delta_{ij}\delta_{kl} + \mu_0(\delta_{ik}\delta_{jl} + \delta_{il}\delta_{jk}), \tag{9}$$

tensor $\mathbf{\Gamma}^0$ admits the following form:

$$\Gamma^0_{ijkl}(\boldsymbol{\xi}) = \frac{1}{4\mu_0}(\delta_{ik}\bar{\xi}_j\bar{\xi}_l + \delta_{il}\bar{\xi}_j\bar{\xi}_k + \delta_{jk}\bar{\xi}_i\bar{\xi}_l + \delta_{jl}\bar{\xi}_i\bar{\xi}_k) - \frac{\lambda_0+\mu_0}{\mu_0(\lambda_0+2\mu_0)}\bar{\xi}_i\bar{\xi}_j\bar{\xi}_k\bar{\xi}_l. \tag{10}$$

In (9,10), δ_{ij} is the usual delta Kronecker symbol and $\bar{\xi}_i$ is the direction cosine of the wave vector $\boldsymbol{\xi}$. By using the definition of the polarization tensor (7) and relation (8), we obtain the integral equation in $\boldsymbol{\epsilon}(\mathbf{x})$:

$$\boldsymbol{\epsilon}(\mathbf{x}) = \mathbf{E} - \mathbf{\Gamma}^0 * (\mathbb{C}(\mathbf{x}) - \mathbb{C}^0) : \boldsymbol{\epsilon}(\mathbf{x}). \tag{11}$$

The transformation of (11) into an equation for eigenstrain $\boldsymbol{\epsilon}^*$ is straightforward by making use of the relations defining the eigenstrain $\boldsymbol{\epsilon}^*$:

$$\begin{aligned} &\boldsymbol{\sigma} = \mathbb{C}^0 : [\boldsymbol{\epsilon}(\mathbf{x}) - \boldsymbol{\epsilon}^*(\mathbf{x})], \\ &\text{or equivalently} \quad (\mathbb{C}^0 - \mathbb{C}(\mathbf{x})) : \boldsymbol{\epsilon}(\mathbf{x}) = \mathbb{C}^0 : \boldsymbol{\epsilon}^*(\mathbf{x}) = -\boldsymbol{\sigma}^*. \end{aligned} \tag{12}$$

Finally, we obtain the same equation as that reported by Nemat-Nasser et al. (1982):

$$\mathbb{C}^0 : \boldsymbol{\epsilon}^*(\mathbf{x}) = (\mathbb{C}^0 - \mathbb{C}(\mathbf{x})) : \left[\mathbf{E} + \sum_{\boldsymbol{\xi}\neq\mathbf{0}} e^{i\boldsymbol{\xi}.\mathbf{x}}\mathbf{\Gamma}^0(\boldsymbol{\xi}) : \mathbb{C}^0 : \boldsymbol{\epsilon}^*(\boldsymbol{\xi})\right]. \tag{13}$$

2.2. Estimations of effective elasticity tensors based on integral equations

From now on, we consider the specific case of a matrix-inclusion composite where each phase is isotropic with elasticity tensors and Lamé constants being $\mathbb{C}^m, \lambda_m, \mu_m$ (matrix), and $\mathbb{C}^i, \lambda_i, \mu_i$ (inclusion). Following the NIH procedure (Nemat-Nasser et al., 1982), we shall estimate the effective elastic properties on the basis of integral equation (13). Taking the matrix as the reference material, that is, $\mathbb{C}^0 = \mathbb{C}^m$ and averaging both sides of (13) over the inclusion

volume Ω with fraction $f = \Omega/V$ yields

$$\mathbb{C}^m : \langle \boldsymbol{\epsilon}^*(\mathbf{x}) \rangle_\Omega = (\mathbb{C}^m - \mathbb{C}^i) : \left[\mathbf{E} + \sum_{\boldsymbol{\xi} \neq \mathbf{0}} \langle e^{i\boldsymbol{\xi}.\mathbf{x}} \rangle_\Omega \boldsymbol{\Gamma}^m(\boldsymbol{\xi}) : \mathbb{C}^m : \boldsymbol{\epsilon}^*(\boldsymbol{\xi}) \right]. \quad (14)$$

Nemat-Nasser et al. (1982) noted that the eigenstrain vanishes outside the inclusion and thus proposed the following approximate evaluation of $\boldsymbol{\epsilon}^*(\boldsymbol{\xi})$:

$$\boldsymbol{\epsilon}^*(\boldsymbol{\xi}) = f \langle \boldsymbol{\epsilon}^*(\mathbf{x}) e^{-i\boldsymbol{\xi}.\mathbf{x}} \rangle_\Omega \simeq f \langle \boldsymbol{\epsilon}^*(\mathbf{x}) \rangle_\Omega \langle e^{-i\boldsymbol{\xi}.\mathbf{x}} \rangle_\Omega. \quad (15)$$

By defining the following shape functions $I(\boldsymbol{\xi})$ and $P(\boldsymbol{\xi})$

$$I(\boldsymbol{\xi}) = \Omega \left\langle e^{i\boldsymbol{\xi}.\mathbf{x}} \right\rangle_\Omega, \quad P(\boldsymbol{\xi}) = \frac{f}{\Omega^2} I(\boldsymbol{\xi}) I(-\boldsymbol{\xi}), \quad (16)$$

and applying the approximation (15) to (14), we obtain

$$\mathbb{C}^m : \langle \boldsymbol{\epsilon}^*(\mathbf{x}) \rangle_\Omega \simeq (\mathbb{C}^m - \mathbb{C}^i) : [\mathbf{E} + \boldsymbol{\Upsilon} : \mathbb{C}^m : \langle \boldsymbol{\epsilon}^*(\mathbf{x}) \rangle_\Omega], \quad (17)$$

where the tensor $\boldsymbol{\Upsilon}$ is the following lattice sum in the reciprocal space:

$$\boldsymbol{\Upsilon} = \sum_{\boldsymbol{\xi} \neq \mathbf{0}} P(\boldsymbol{\xi}) \boldsymbol{\Gamma}^m(\boldsymbol{\xi}). \quad (18)$$

Inverting (17) yields the average eigenstrain $\langle \boldsymbol{\epsilon}^*(\mathbf{x}) \rangle_\Omega$

$$\langle \boldsymbol{\epsilon}^*(\mathbf{x}) \rangle_\Omega = \left[(\mathbb{C}^m - \mathbb{C}^i)^{-1} : \mathbb{C}^m - \boldsymbol{\Upsilon} : \mathbb{C}^m \right]^{-1} : \mathbf{E}. \quad (19)$$

Next, we average (12) with the matrix as the reference material, and we find the relation between $\mathbf{E}$, $\boldsymbol{\Sigma}$, and $\langle \boldsymbol{\epsilon}^*(\mathbf{x}) \rangle_\Omega$:

$$\boldsymbol{\Sigma} = \mathbb{C}^m : (\mathbf{E} - \langle \boldsymbol{\epsilon}^*(\mathbf{x}) \rangle_V), \quad \text{or} \quad \boldsymbol{\Sigma} = \mathbb{C}^m : (\mathbf{E} - f \langle \boldsymbol{\epsilon}^*(\mathbf{x}) \rangle_\Omega). \quad (20)$$

Finally, comparing (20) with (3) and accounting for (19), we can derive the overall tensor $\mathbb{C}^e$:

$$\mathbb{C}^e = \mathbb{C}^m - f\left[(\mathbb{C}^m - \mathbb{C}^i)^{-1} - \boldsymbol{\Upsilon}\right]^{-1}. \tag{21}$$

The success of the NIH estimation relies on the accuracy of Eq. (15). Theoretically speaking, if the inclusions have an ellipsoidal shape and occupy a sufficiently small volume fraction f, approximation (15) is valid. Indeed, Eshelby (1957) proved that the stress/strain fields inside an ellipsoidal inclusion embedded in an infinite matrix and subject to homogeneous stress/strain boundary conditions at infinity are also homogeneous. For interacting inclusions, the inclusion stress/strain fields are no longer uniform, although (15) is still expected to yield accurate results for a large range of volume fractions.

2.3. Tensor $\boldsymbol{\Upsilon}$ and its relation with the periodic Eshelby tensor

The periodic Eshelby problem can also be addressed, where the inclusions in the above study are made of the same material as the matrix (i.e., $\mathbb{C}^i = \mathbb{C}^m$) but are subjected to a uniform eigenstrain $\boldsymbol{\epsilon}^* = \mathbf{E}^*$ inside their domains Ω. Different from the classical Eshelby problems, the strain field inside each inclusion is generally not uniform. However, if we average this strain field over each inclusion, we can still define the periodic Eshelby tensor $\mathbb{S}^p$ as follows:

$$\langle \boldsymbol{\epsilon}(\mathbf{x}) \rangle_\Omega = \mathbb{S}^p : \mathbf{E}^*, \tag{22}$$

As strain field $\boldsymbol{\epsilon}$ can be computed from $\boldsymbol{\epsilon}^*$ via (8,12) with relation (15) becoming exact, this tensor can be determined by

$$\mathbb{S}^p = \sum_{\boldsymbol{\xi} \neq \mathbf{0}} P(\boldsymbol{\xi}) \boldsymbol{\Gamma}^m(\boldsymbol{\xi}) : \mathbb{C}^m. \tag{23}$$

It is clear that if the domain V is sufficiently large compared with the size of the inclusion, $\mathbb{S}^p$ should be equal to the classical Eshelby tensor $\mathbb{S}^\infty$. Nev-

ertheless, there is always a simple connection between $\mathbb{S}^p$ and $\boldsymbol{\Upsilon}$:

$$\mathbb{S}^p = \boldsymbol{\Upsilon} : \mathbb{C}^m. \tag{24}$$

This leads to an alternative interpretation of NIH approximation: *the NIH approximation corresponds to an estimation of the mean strain over the inclusions produced by the periodic Eshelby tensor*. From (24), we find that the tensor $\boldsymbol{\Upsilon}$ plays the same role as the classical Hill tensor, but here in the periodic setting. This "periodic Hill tensor" provides the average deformation inside the inclusions due to a constant polarization field.[1]

On returning to our original problem, combining (74) with (10), this tensor $\boldsymbol{\Upsilon}$ can be written as follows:

$$\boldsymbol{\Upsilon} = \frac{1}{2\mu_m}\mathbb{W} - \frac{\lambda_m + \mu_m}{\mu_m(\lambda_m + 2\mu_m)}\mathbb{U} \tag{25}$$

where $\mathbb{W}$ and $\mathbb{U}$ are fourth-order tensors that depend only on the geometry.

In the following, the unit cell is assumed to be symmetrical with respect to three orthogonal planes. Under this condition, the matrix representations of $\mathbb{W}$ and $\mathbb{U}$ are given in Kelvin's notation by:

$$[\mathbb{W}] = \begin{bmatrix} 2S_1 & 0 & 0 & 0 & 0 & 0 \\ 0 & 2S_2 & 0 & 0 & 0 & 0 \\ 0 & 0 & 2S_3 & 0 & 0 & 0 \\ 0 & 0 & 0 & S_2 + S_3 & 0 & 0 \\ 0 & 0 & 0 & 0 & S_3 + S_1 & 0 \\ 0 & 0 & 0 & 0 & 0 & S_1 + S_2 \end{bmatrix} \tag{26}$$

[1]The classical Hill tensor, frequently used in micromechanics, is defined as the product between the compliance tensor $(\mathbb{C}^m)^{-1}$ and the classical Eshelby tensor $\mathbb{S}^\infty$ (Hill, 1965)

and

$$[\mathbb{U}] = \begin{bmatrix} S_4 & S_9 & S_8 & 0 & 0 & 0 \\ S_9 & S_5 & S_7 & 0 & 0 & 0 \\ S_8 & S_7 & S_6 & 0 & 0 & 0 \\ 0 & 0 & 0 & 2S_7 & 0 & 0 \\ 0 & 0 & 0 & 0 & 2S_8 & 0 \\ 0 & 0 & 0 & 0 & 0 & 2S_9 \end{bmatrix} \tag{27}$$

where S_i with $i = 1, 2, .., 9$ are the lattice sums given by

$$S_i = \sum_{\boldsymbol{\xi} \neq \mathbf{0}} P(\boldsymbol{\xi}) \bar{\xi}_i^2, \quad S_{i+3} = \sum_{\boldsymbol{\xi} \neq \mathbf{0}} P(\boldsymbol{\xi}) \bar{\xi}_i^4, \quad S_{i+6} = \sum_{\boldsymbol{\xi} \neq \mathbf{0}} P(\boldsymbol{\xi}) \bar{\xi}_j^2 \bar{\xi}_k^2,$$
$$i, j, k = 1, 2, 3, \quad i \neq j \neq k \neq i. \tag{28}$$

These lattice sums are not independent because of the relation $\bar{\xi}_2^2 + \bar{\xi}_2^2 + \bar{\xi}_3^2 = 1$, which leads to three relations:

$$S_{i+3} + S_{j+6} + S_{k+6} = S_i, \quad i, j, k = 1, 2, 3, \quad i \neq j \neq k \neq i. \tag{29}$$

It implies that only six of these lattice sums are independent and that not all of the elastic constants are independent, as shown, for example, by Cohen (2004) in the cubic case. It is worth noting that the symmetry of the effective tensor is the same as that of tensor $\boldsymbol{\Upsilon}$ and that this tensor is orthotropic, which corresponds to the symmetry assumptions on the periodic cell. To obtain the overall elasticity tensor, we need to invert $(\mathbb{C}^m - \mathbb{C}^i)^{-1} - \boldsymbol{\Upsilon}$ in (21). These tensors can be inverted through lengthy expressions for a general distribution with orthotropic symmetry (Luciano and Barbero, 1994). Further, in some special cases (for example, cubic symmetries), we can obtain simple analytical expressions, as recalled thereafter.

3. Closed-form expressions for effective tensors in the case of inclusions centered on periodic lattices

3.1. Lattice sum computation and integral approximation

Before obtaining the effective properties, the method for analytical estimation of the lattice sums S_i with $i = 1, 2, .., 9$ is introduced in the general form

$$\sum_{\boldsymbol{\eta}\neq\mathbf{0}} \bar{\eta}_i^{2\alpha}\bar{\eta}_j^{2\beta} H(\boldsymbol{\eta}), \quad i,j = 1,2,3 \tag{30}$$

with

$$\boldsymbol{\eta} = R\boldsymbol{\xi}, \quad H(\boldsymbol{\eta}) = P(\boldsymbol{\xi}), \quad \bar{\boldsymbol{\eta}} = \frac{\boldsymbol{\eta}}{\eta}, \eta = |\boldsymbol{\eta}|. \tag{31}$$

Here, α and β are non negative integers and R is the inclusion characteristic length used to generate the dimensionless wave vectors $\boldsymbol{\eta}$ from $\boldsymbol{\xi}$. It is noted that the $\boldsymbol{\eta}$ points form a rectangular lattice in three-dimensional (3D) space with density:

$$\rho = \frac{a_1 a_2 a_3}{(2\pi R)^3}. \tag{32}$$

If $H(\boldsymbol{\eta})$ is a decaying function of η, we can reasonably estimate the sum

$$\sum_{\boldsymbol{\xi}\in D} \bar{\eta}_i^{2\alpha}\bar{\eta}_j^{2\beta} H(\boldsymbol{\eta}) \simeq \rho \int_D \bar{\xi}_i^{2\alpha}\bar{\xi}_j^{2\beta} H(\boldsymbol{\eta}) d\boldsymbol{\eta}, \tag{33}$$

for a sufficiently remote and large region D where $H(\boldsymbol{\eta})$ varies slowly. As a result, the infinite lattice sum can be estimated by a finite sum of several leading terms and a continuous integral for longer wave vectors, for example,

$$\sum_{\boldsymbol{\eta}\neq\mathbf{0}} \bar{\eta}_i^{2\alpha}\bar{\eta}_j^{2\beta} H(\boldsymbol{\eta}) \simeq \sum_{|\boldsymbol{\eta}|<\eta_c} \bar{\eta}_i^{2\alpha}\bar{\eta}_j^{2\beta} H(\boldsymbol{\eta}) + \rho \int_{\eta_c}^{\infty} H(\boldsymbol{\eta})\bar{\eta}_i^{2\alpha}\bar{\eta}_j^{2\beta} d\boldsymbol{\eta}. \tag{34}$$

The cutoff radius η_c in (34) determines the number of leading terms from the series that are retained in the new formula. In many cases where $H(\boldsymbol{\eta})$ depends on its modulus η alone, we can calculate the integral in the right-

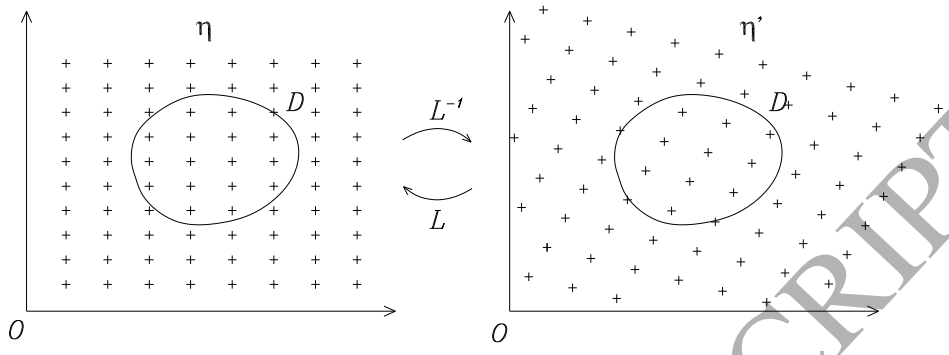

Figure 1: Grid $\boldsymbol{\eta}$ and $\boldsymbol{\eta}'$ in Fourier space

hand side (RHS) of (34):

$$\rho \int_{\eta_c}^{\infty} H(\eta) \bar{\eta}_i^{2\alpha} \bar{\eta}_j^{2\beta} d\boldsymbol{\eta} = \rho \int_{\eta_c}^{\infty} H(\eta) \eta^2 d\eta \int_{|\eta|=1} \bar{\eta}_i^{2\alpha} \bar{\eta}_j^{2\beta} dS \tag{35}$$

The second integral of the RHS involving the unit sphere surface $|\eta| = 1$ can be evaluated analytically in numerous cases. The first integral can also be computed if the explicit expression of $H(\eta)$ is known. For example, the simple cubic distribution of spherical inclusions studied in the next section corresponds to the following expression of $H(\boldsymbol{\eta})$:

$$H(\boldsymbol{\eta}) = f\varphi(\eta), \quad \varphi(\eta) = \frac{9[\sin(\eta) - \eta\cos(\eta)]^2}{\eta^6}. \tag{36}$$

The associated integrals involving $H(\boldsymbol{\eta})$ can be computed by

$$\rho \int_{\eta_c}^{\infty} H(\eta) \eta^2 d\eta = 9\rho f J(\eta_c) \tag{37}$$

where

$$J(\eta) = \frac{\pi}{6} - \frac{\cos 2\eta}{6\eta} - \frac{1}{3}\mathrm{Si}(2\eta) + \frac{1}{2\eta} + \frac{1}{6\eta^3} - \frac{\sin 2\eta}{3\eta^2} - \frac{\cos 2\eta}{6\eta^3} \tag{38}$$

and $\mathrm{Si}(\eta)$ is the sine integral

$$\mathrm{Si}(\eta) = \int_0^{\eta} \frac{\sin \eta'}{\eta'} d\eta'. \tag{39}$$

The above summation method can be extended to the more general cases where $H(\boldsymbol{\eta})$ is the function of the modulus $|\mathbf{L}^{-1}.\boldsymbol{\eta}|$ with $\mathbf{L}^{-1}$ being any linear transformation. Indeed, by simply posing

$$\boldsymbol{\eta}' = \mathbf{L}^{-1}.\boldsymbol{\eta}, \quad H(\boldsymbol{\eta}) = H'(\eta'), \tag{40}$$

we can calculate the sum using grid $\boldsymbol{\eta}'$ as follows:

$$\sum_{\boldsymbol{\eta}' \neq \mathbf{0}} \frac{(L_{ik}\eta'_k)^{2\alpha}(L_{jl}\eta'_l)^{2\beta} H'(\eta')}{[(L_{1k}\eta'_k)^2 + (L_{2k}\eta'_k)^2 + (L_{3k}\eta'_k)^2]^{\alpha+\beta}} \tag{41}$$

We can keep several leading terms by using the radius η'_c and estimating the remaining series with an integral. The integral estimation method introduced previously can be applied as the grid $\boldsymbol{\eta}'$ is obtained from $\boldsymbol{\eta}$ by a homogeneous deformation $\mathbf{L}^{-1}$; thus, the grid $\boldsymbol{\eta}'$ is also uniform. The only difference now is to compute the integral on the unit sphere surface. Taking the example of an ellipsoidal inclusion studied in the next section, we have

$$H(\boldsymbol{\eta}) = f\varphi(\eta'), \quad \eta' = \sqrt{\eta_1^2/\chi_1^2 + \eta_2^2/\chi_2^2 + \eta_2^2/\chi_2^2} \tag{42}$$

where χ_i are dilatation coefficients. The associated surface integral becomes

$$\int_{|\eta'|=1} \frac{(\chi_i\eta'_i)^{2\alpha}(\chi_j\eta'_j)^{2\beta}}{[(\chi_1\eta'_1)^2 + (\chi_2\eta'_2)^2 + (\chi_3\eta'_3)^2]^{\alpha+\beta}} dS, \quad i,j \text{ not summed} \tag{43}$$

which can yield closed-form solutions in numerous cases.

Finally, we note that if the ratio $R/a_i \to 0 \ \ \forall i = 1,2,3$, the $\boldsymbol{\eta}$ grid becomes infinitely dense. As a result, the relation (33) must hold for all domain D,

and the infinite lattice sum is equivalent to the integral over the whole space:

$$\sum_{\boldsymbol{\eta}\neq\mathbf{0}} \bar{\eta}_i^{2\alpha}\bar{\eta}_j^{2\beta} H(\boldsymbol{\eta}) = \int \bar{\eta}_i^{2\alpha}\bar{\eta}_j^{2\beta} H(\boldsymbol{\eta})\rho d\boldsymbol{\eta}. \tag{44}$$

Although $\rho \to \infty$, the product $H(\boldsymbol{\eta})\rho$ is generally bounded for the cases examined in the later section. As a result, the integral in RHS of (44) is well defined. Further, one can also expect to recover analytical results corresponding to the infinite volume domain limit.

3.2. Cubic lattice arrangements

In this subsection, we consider microstructures composed of identical spheres of radius R arranged in a cubic lattice of period a (see Fig. 2). We note that the Fourier transform of the indicator function of a spherical inclusion of radius R located at $\mathbf{x}_c$ admits the simple closed form

$$\int_{V_s} e^{i\boldsymbol{\xi}.\mathbf{x}} d\mathbf{x} = 3V_s \frac{\sin\eta - \eta\cos\eta}{\eta^3} e^{i\boldsymbol{\xi}.\mathbf{x}_c}, \quad V_s = \frac{4\pi R^3}{3}, \quad \eta = \xi R. \tag{45}$$

Using the elementary result (45), one can determine $I(\boldsymbol{\xi})$ and $P(\boldsymbol{\xi})$ for any distribution of spheres inside the unit cell. For cubic crystal system arrangements (see Fig. 2), To et al. (2013) derived the following expressions for $P(\boldsymbol{\xi})$ (or equivalently $H(\boldsymbol{\eta})$):

$$P(\boldsymbol{\xi}) = H(\boldsymbol{\eta}) = \alpha f \varphi(\eta), \tag{46}$$

with $\varphi(\eta)$ being defined in (36). The coefficient α depends on the geometry, equal to 1 for simple cubic arrangement. For other arrangements, it can be computed as follows:

- Body-centered cubic (BCC)

$$\alpha = 1 \text{ if } n_1 + n_2 + n_3 \text{ is even, otherwise } \alpha = 0, \tag{47}$$

- Face-centered cubic (FCC)

$$\alpha = 1 \text{ if } n_1, n_2, n_3 \text{ are all even or odd, otherwise } \alpha = 0. \quad (48)$$

Due to the symmetry of the cell and the definition of $P(\boldsymbol{\xi})$ in (16), the lattice sums present the equalities

$$S_1 = S_2 = S_3, \quad S_4 = S_5 = S_6, \quad S_7 = S_8 = S_9,$$

whereas S_1, S_4, and S_7 are linked via the property

$$S_4 + 2S_7 = S_1. \quad (49)$$

As a result, $\boldsymbol{\Upsilon}$ is a cubic tensor and one can easily compute the effective tensor $\mathbb{C}^e$ from the results of Appendix A.

- The effective bulk modulus κ_e is determined by

$$\kappa^e = \kappa_m - \frac{f}{\frac{1}{\kappa_m - \kappa_i} - \frac{9S_3}{3\kappa_m + 4\mu_m}} \quad (50)$$

- The first and the second effective shear modulus μ^e and μ^{e*} are determined by

$$\mu^e = \mu_m - \frac{f(\mu_i - \mu_m)}{1 - \beta}, \quad \mu^{e*} = \mu_m - \frac{f(\mu_i - \mu_m)}{1 - \beta^*} \quad (51)$$

where the coefficients β and β^* are defined as

$$\begin{aligned} \beta &= \frac{2(\mu_i - \mu_m)}{\mu_m} \cdot \frac{(3\kappa_m + 4\mu_m)S_1 - 2(3\kappa_m + \mu_m)S_7}{3\kappa_m + 4\mu_m} \\ \beta^* &= \frac{6(\mu_i - \mu_m)}{\mu_m} \cdot \frac{\mu_m S_4 + 3\left(\kappa_m + \mu_m\right) S_7}{3\kappa_m + 4\mu_m} \end{aligned} \quad (52)$$

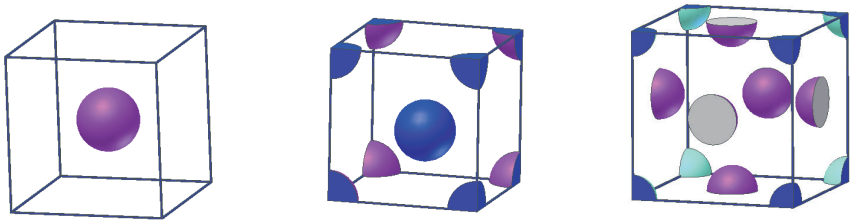

Figure 2: Unit cell of cubic lattice structures (from left to right: simple cubic, body-centered cubic, and face-centered cubic)

It is worth noting that these expressions are identical in form to those given by Cohen (2004). Using this latter work, the terms depending on the geometry and concentration are given by

$$S_1 = \frac{1-f}{3}, \tag{53}$$

$$S_4 = \frac{1}{5}[1 - f - 2(A_1 f + A_2 f^{5/3})], \tag{54}$$

$$S_7 = \frac{1}{15}[1 - f + 3(A_1 f + A_2 f^{5/3})], \tag{55}$$

where A_1 and A_2 are coefficients depending on the geometry that characterize the kind of lattice up to second order. They were computed by Cohen (2004). This shows the very similarity between the present approach and that of Cohen (2004) despite the difference in nature. It is clear that the result of Cohen (2004) is easier to use than ours, because the expressions for S_1, S_4 and S_7 are the same for any cubic lattice of the same kind. However, as shown subsequently, the previously described results and their expressions in closed forms that are described thereafter can be extended readily to other geometries of the microstructure.

Equations (50–51) can be further simplified by evaluating the lattice sums S_1, S_4, and S_7 analytically using the method described in subsection 3.1 with

grid density $\rho = a^3/8\pi^3R^3$. It has been previously reported that S_7 can be easily computed from S_1 and S_4 via relation (49). For BCC and FCC arrangements, due to the fluctuation of α (see Eqs. 47 and 48), $H(\boldsymbol{\eta})$ in the integral (34) should be replaced by its average $\bar{H}(\eta)$. Generally, we have

$$\bar{H}(\eta) = \bar{\alpha} f \varphi(\eta) \tag{56}$$

where $\bar{\alpha} = 1$(SC), $\frac{1}{2}$(BCC) and $\frac{1}{4}$(FCC). However, we note that the composite coefficient

$$\rho \bar{\alpha} f = \frac{1}{2\pi^2} \tag{57}$$

is independent of the microstructure, leading to a unique expression for the long wave integral

$$\rho \int_{\eta_c}^{\infty} \bar{H}(\eta)\eta^2 d\eta = \frac{3}{2\pi^2} J(\eta_c) \tag{58}$$

Assuming $\epsilon = 2\pi R/a$, the expressions of S_1 and S_4 for different cubic systems are finally presented by keeping the first terms of the lattice sums. The numerical evidence shows that keeping four to six leading terms produces satisfying results. The terms that are kept corresponding to the value of η_c are given as follows:

- Simple cubic system (SC) with $\eta_c = 2\epsilon$

$$\begin{aligned} S_1 &= \frac{2}{\pi} J(2\epsilon) + f[2\varphi(\epsilon) + 4\varphi(\sqrt{2}\epsilon) + \frac{8}{3}\varphi(\sqrt{3}\epsilon) + 2\varphi(2\epsilon)], \\ S_4 &= \frac{6}{5\pi} J(2\epsilon) + f[2\varphi(\epsilon) + 2\varphi(\sqrt{2}\epsilon) + \frac{8}{9}\varphi(\sqrt{3}\epsilon) + 2\varphi(2\epsilon)]. \end{aligned} \tag{59}$$

- BCC with $\eta_c = \sqrt{12}\epsilon$

$$
\begin{aligned}
S_1 &= \frac{2}{\pi} J(\sqrt{12}\epsilon) + f[4\varphi(\sqrt{2}\epsilon) + 2\varphi(2\epsilon) + 8\varphi(\sqrt{6}\epsilon) + 4\varphi(\sqrt{8}\epsilon) + \\
&\quad + 8\varphi(\sqrt{10}\epsilon) + \frac{8}{3}\varphi(\sqrt{12}\epsilon)], \\
S_4 &= \frac{6}{5\pi} J(\sqrt{12}\epsilon) + f[2\varphi(\sqrt{2}\epsilon) + 2\varphi(2\epsilon) + 4\varphi(\sqrt{6}\epsilon) + 2\varphi(\sqrt{8}\epsilon) + \\
&\quad + \frac{164}{25}\varphi(\sqrt{10}\epsilon) + \frac{8}{9}\varphi(\sqrt{12}\epsilon)].
\end{aligned} \tag{60}
$$

- FCC with $\eta_c = 4\epsilon$

$$
\begin{aligned}
S_1 &= \frac{2}{\pi} J(4\epsilon) + f[\frac{8}{3}\varphi(\sqrt{3}\epsilon) + 2\varphi(2\epsilon) + 4\varphi(\sqrt{8}\epsilon) + 8\varphi(\sqrt{11}\epsilon) \\
&\quad + \frac{8}{3}\varphi(\sqrt{12}\epsilon) + 2\varphi(4\epsilon)], \\
S_4 &= \frac{6}{5\pi} J(4\epsilon) + f[\frac{8}{9}\varphi(\sqrt{3}\epsilon) + 2\varphi(2\epsilon) + 2\varphi(\sqrt{8}\epsilon) + \frac{664}{121}\varphi(\sqrt{11}\epsilon) \\
&\quad + \frac{8}{9}\varphi(\sqrt{12}\epsilon) + 2\varphi(4\epsilon)].
\end{aligned} \tag{61}
$$

The maximal relative difference between the analytical expressions and the full lattice sums is 2% (see Fig. 3). For FCC and BCC, more leading terms than in the SC case are retained to achieve the high precision level, due to the fluctuation of the coefficient α. Using four leading terms for FCC and BCC cases can result in a simpler expression but a higher maximal error (up to 8%). Even if this error was found to have a small impact on the effective properties in the case of thermal conduction, we shall use the accurate expressions (60,61) in the remaining part of the paper.

As mentioned earlier (see Eq. 44), when the ratio $R/a \to 0$ and $f \to 0$, we obtain the limit that is independent of the microstructure and volume

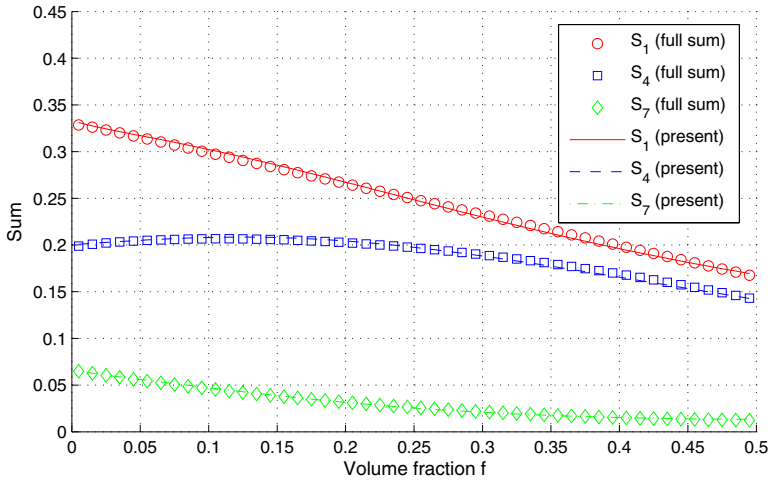

Figure 3: Comparison between the full lattice sums with resolution $-128 < n_i \leq 128$ and Eq. (59) for the simple cubic case. At $f = 0$, the lattice sums take the limit values $S_1 = 1/3$, $S_4 = 1/5$, and $S_7 = 1/15$.

fraction f:

$$S_1 = \frac{2}{\pi} J(0) = \frac{1}{3}, \quad S_4 = \frac{6}{5\pi} J(0) = \frac{1}{5}. \tag{62}$$

This interesting property can be explained in relation to the Eshelby tensor for periodic spheres discussed in Section 2.3 (which becomes equal to the classical Eshelby tensor in the dilute case), as also observed in Fig. 3.

3.3. Orthorhombic arrangements of spheres

As will be seen thereafter in the numerical examples, the previously described closed-form solution for the effective properties of cubic lattices leads to results that are very similar to those of Cohen (2004). In addition, this earlier solution is expressed by simple expressions of the effective elasticity tensor. Thus, in this section and the following, we show that the solution described in the previous subsection can be readily extended to other kinds

of periodic cells.

First, the case of an array of spheres with orthorhombic symmetry is considered, the center of the spheres being lattice points of an orthorhombic lattice characterized by a_1, a_2, a_3, with $a_1 \neq a_2 \neq a_3 \neq a_1$. In this case, the effective elasticity tensor is again given by expression (21). It can be seen that all tensors appearing in this expression are isotropic except the orthotropic tensor $\boldsymbol{\Upsilon}$ that is characterized by the symmetry of the lattice. Expressions for all effective elasticity components are explicit, but cumbersome, as a 3×3 matrix needs to be inverted, except for the shear components that are listed below:

$$C^e_{jkjk} = \mu_m - \frac{f\mu_m}{\frac{\mu_m}{\mu_m-\mu_i} - (S_j + S_k) + 4\frac{\lambda_m+\mu_m}{\lambda_m+2\mu_m}S_{i+6}}, \quad i,j,k = 1,2,3, \quad i \neq j \neq k \neq i. \tag{63}$$

Regarding the computation of the lattice sum S_i, it is clear that the continuous integral estimation of the remaining series is identical to the cubic lattice case, except for the density that is now given by the general expression (32). This implies that the contribution of longer wave vectors to the sum does not contribute to the orthotropic anisotropy of the material. The related anisotropic terms are contained in the complementary finite sum, and the number of independent terms to keep in the finite sum is usually higher than in the case of the cubic lattice.

The infinite sum in (63) can be computed as follows:

$$S_i = \frac{2}{\pi}J(\eta_c) + f\sum_{\eta<\eta_c} \bar{\eta}_i^2 \alpha\varphi(\eta), \quad S_{i+6} = \frac{2}{5\pi}J(\eta_c) + f\sum_{\eta<\eta_c} \bar{\eta}_j^2\bar{\eta}_k^2 \alpha\varphi(\eta), \quad i,j,k = 1,2,3, \quad i \neq j \neq k \neq i \tag{64}$$

The lattice sums S_4, S_5, and S_6 contributing to the effective components other than C^e_{2323}, C^e_{1313}, and C^e_{1212} are given as follows for completeness:

$$S_{i+3} = \frac{6}{5\pi} J(\eta_c) + f \sum_{\eta<\eta_c} \bar{\eta}_i^4 \alpha\varphi(\eta), \quad i = 1, 2, 3. \tag{65}$$

The coefficient α is a function of n_1, n_2, n_3 with the same meaning as in (47,48). It can be translated to the SO, BCO, and FCO cases.

3.4. Orthorhombic arrangements of ellipsoids

For an ellipsoid of principal radii $R/\chi_1, R/\chi_2$, and R/χ_3 located at $\mathbf{x}_c$, we know the elementary result

$$\begin{aligned} &\int_{V_e} e^{i\boldsymbol{\xi}\cdot\mathbf{x}} d\mathbf{x} = 3V_e \frac{\sin\eta' - \eta'\cos\eta'}{\eta'^3} e^{i\boldsymbol{\xi}\cdot\mathbf{x}_c}, \quad V_e = \frac{4\pi R^3}{3\chi_1\chi_2\chi_3}, \\ &\eta' = (\eta_1^2/\chi_1^2 + \eta_2^2/\chi_2^2 + \eta_3^2/\chi_3^2)^{1/2}, \quad \boldsymbol{\eta} = R\boldsymbol{\xi}. \end{aligned} \tag{66}$$

Again, the procedure described in subsection 3.1 is used to obtain the analytical solution. Assuming that the ellipsoid is located at the center of the rectangular cuboid of dimension $a_1 \times a_2 \times a_3$ and performing the transformation $\eta'_1 = \eta_1/\chi_1$,$\eta'_2 = \eta_2/\chi_2$ and $\eta'_3 = \eta_3/\chi_3$, the lattice sums can now be evaluated by

$$\begin{aligned} S_i &= \frac{3}{2\pi^2} T_i J(\eta'_c) + f \sum_{\eta'<\eta'_c} \frac{\eta_i'^2\chi_i^2}{\eta_1'^2\chi_1^2 + \eta_2'^2\chi_2^2 + \eta_3'^2\chi_3^2} \alpha\varphi(\eta'), \\ S_{i+3} &= \frac{3}{2\pi^2} T_{i+3} J(\eta'_c) + f \sum_{\eta'<\eta'_c} \left[\frac{\eta_i'^2\chi_i^2}{\eta_1'^2\chi_1^2 + \eta_2'^2\chi_2^2 + \eta_3'^2\chi_3^2}\right]^2 \alpha\varphi(\eta'), \\ S_{i+6} &= \frac{3}{2\pi^2} T_{i+6} J(\eta'_c) + f \sum_{\eta'<\eta'_c} \frac{\eta_j'^2\chi_j^2\eta_k'^2\chi_k^2}{[\eta_1'^2\chi_1^2 + \eta_2'^2\chi_2^2 + \eta_3'^2\chi_3^2]^2} \alpha\varphi(\eta'), \\ &i, j, k = 1, 2, 3, \quad i \neq j \neq k \neq i. \end{aligned} \tag{67}$$

The surface integrals on the unit sphere surface T_i are defined by

$$
\begin{aligned}
T_i &= \int_{|\eta'|=1} \frac{(\chi_i \eta_i')^2 dS}{[(\chi_1\eta_1')^2 + (\chi_2\eta_2')^2 + (\chi_3\eta_3')^2]} \\
T_{i+3} &= \int_{|\eta'|=1} \frac{(\chi_i \eta_i')^4 dS}{[(\chi_1\eta_1')^2 + (\chi_2\eta_2')^2 + (\chi_3\eta_3')^2]^2} \\
T_{i+6} &= \int_{|\eta'|=1} \frac{(\chi_j \eta_j')^2 (\chi_k \eta_k')^2 dS}{[(\chi_1\eta_1')^2 + (\chi_2\eta_2')^2 + (\chi_3\eta_3')^2]^2}, \\
& i,j,k = 1,2,3, \quad i \neq j \neq k \neq i.
\end{aligned} \tag{68}
$$

Regarding the cutoff radius η_c' in function of ϵ, it can be set to the same value as η_c in (59) with $\epsilon = \max(2\pi R/\chi_1 a_1, 2\pi R/\chi_2 a_2, 2\pi R/\chi_3 a_3)$. It is interesting to note that if $\chi_1 a_1 = \chi_2 a_2 = \chi_3 a_3$, that is, if the ellipsoid and the unit cell have the same aspect ratio, the grid $\boldsymbol{\eta}'$ is a cubic grid and the leading terms kept in the series are as simple as for the cubic lattice cases (59–61). Figure 4 is an example showing that the analytical expression for the FCO arrangement is highly accurate, compared to the full computation of the lattice sums.

It can be shown that T_1, T_2, and T_3 are expressed as functions of elliptical integrals (see, e.g., Eshelby, 1957; Mura, 1987). Assuming that $\chi_1 < \chi_2 < \chi_3$, these integrals read

$$
\begin{aligned}
T_1 &= \frac{4\pi\chi_1^3\chi_2^2\chi_3}{(\chi_2^2-\chi_1^2)\sqrt{\chi_3^2-\chi_1^2}}[F(\theta,k) - E(\theta,k)] \\
T_3 &= \frac{4\pi\chi_1\chi_2^2\chi_3^3}{(\chi_3^2-\chi_2^2)\sqrt{\chi_3^2-\chi_1^2}}\left[\frac{1}{\chi_2}\sqrt{\chi_3^2-\chi_1^2} - E(\theta,k)\right] \\
T_2 &= 4\pi - T_1 - T_3
\end{aligned} \tag{69}
$$

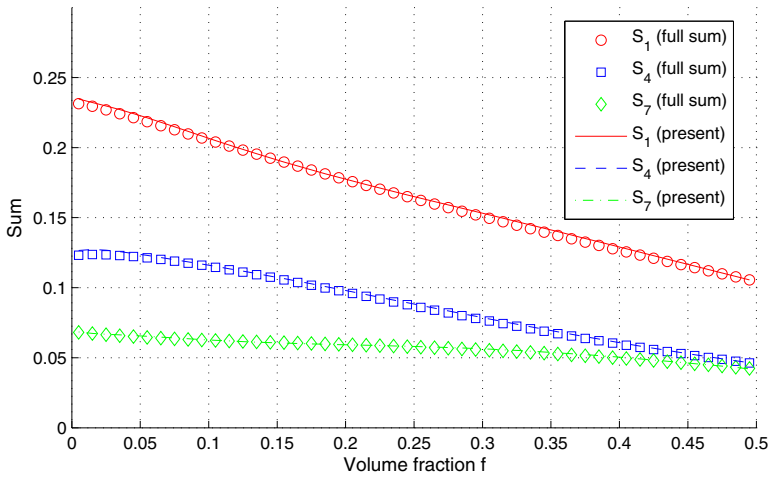

Figure 4: Comparison between the full lattice sums with resolution $-128 < n_i \leq 128$ and Eqs. (67,68) for the FCO case. The spheroids and the unit cell have the same dimension ratio $a \times a \times 0.5a$ and $R \times R \times 0.5R$. The cutoff radius is $\eta_c' = 4\epsilon$ and $\epsilon = 2\pi R/a$. For the sake of clarity, only the sums S_1, S_4 and S_7 are presented.

where

$$F(\theta,k) = \int_0^\theta \frac{dw}{\sqrt{1-k^2\sin^2 w}}, \quad E(\theta,k) = \int_0^\theta \sqrt{1-k^2\sin^2 w}\,dw$$
$$\theta = \arcsin\sqrt{1-\chi_1^2/\chi_3^2}, \quad k = \sqrt{\frac{\chi_3^2(\chi_2^2-\chi_1^2)}{\chi_2^2(\chi_3^2-\chi_1^2)}}. \tag{70}$$

In the general case, there are no available explicit analytical expressions for the remaining integrals T_i, $i = 4, 5, .., 9$ except for spheroidal inclusions. Obviously, only T_i, $i = 4, 5, 6$ are necessary, due to the general relation between S_i. It can be shown that each of these coefficients can be obtained from one simple scalar integral, which is in any case easier to compute than the full lattice sum. The related scalar integrals are provided in Appendix C.

For the case of spheroids where the axes of cylindrical symmetry are ori-

ented along the x_3 axis, we can set $\chi_1 = \chi_2 = 1$ and $\chi_3 = \chi$ and evaluate analytically T_i in spherical coordinates (see Appendix B). The final results are given as follows:

$$
\begin{aligned}
T_1 &= T_2 = \frac{2\pi}{\gamma^3}(\delta\chi^2 - \gamma), \quad T_3 = \frac{4\pi\chi^2}{\gamma^3}(\gamma - \delta) \\
T_4 &= T_5 = \frac{3\pi}{4\gamma^5}(\chi^2(\chi^2 - 4)\delta + \gamma(\chi^2 + 2)), \\
T_6 &= \frac{2\pi\chi^2}{\gamma^5}(\gamma(2\chi^2 + 1) - 3\chi^2\delta) \\
T_7 &= T_8 = \frac{\pi\chi^2}{\gamma^5}((\chi^2 + 2)\delta' - 3\gamma), \\
T_9 &= \frac{\pi}{4\gamma^5}(\chi^2(\chi^2 - 4)\delta + \gamma(\chi^2 + 2)),
\end{aligned} \tag{71}
$$

with $\gamma = \sqrt{\chi^2 - 1}$ and $\delta = \arctan\gamma$ for oblate inclusions ($\chi > 1$) and $\gamma = \sqrt{1 - \chi^2}$ and $\delta = \tanh^{-1}\gamma$ for prolate inclusions ($\chi < 1$).

4. Closed-form expressions for random distributions of spheres or ellipsoids

In the previous sections, we considered only the cases of lattice distributions of spheres and ellipsoids. This section is devoted to random distributions of spheres and ellipsoids. Therefore, the periodic cell now contains a random distribution of aligned inclusions. To proceed, the ergodic media hypothesis (Torquato, 2001) is adopted, that is, the ensemble average results, notation $\langle ... \rangle_{ens}$, are identical results for one sample in the infinite-volume limit. This assumption guarantees the existence and uniqueness of the effective tensor $\mathbb{C}^e$.

Obviously, the ergodic assumption is not sufficient to estimate the effective properties. It is necessary to introduce also probabilistic assumptions on the distributions of inclusions to reach this objective. These assumptions can be

based on the introduction of probability density functions, correlation functions in the real space, but also on quantities defined in Fourier space. Let us consider in a first step the notions defined in the real space that sustain our work. Following Torquato (2001), it is convenient to introduce the probability density function P_N such that $P_N(\mathbf{r}_1, \mathbf{r}_2, ...)d\mathbf{r}_1 d\mathbf{r}_2...$ represents the probability of finding the center of inclusion 1 in $d\mathbf{r}_1$, the center of inclusion 2 in $d\mathbf{r}_2$,... By a convenient partial integration of this probability function, the pair correlation function can be simplified into the radial distribution function $g_2(r_{12})$ (with $r_{12} = ||\mathbf{r}_2 - \mathbf{r}_1||$) under the assumption of statistical isotropy.

However, our method uses quantities defined in Fourier space and it is possible to define also ensemble average on functions defined in Fourier space. So, in a first step, such functions will be defined. In a second step the link between such ensemble averages and the radial distribution function g_2 defined by using the full probabilistic machinery will be provided.

As a result of the ergodic assumption, from (20), we can find that the following relation must hold true:

$$\langle \boldsymbol{\epsilon}^*(\mathbf{x}) \rangle_\Omega = \langle \langle \boldsymbol{\epsilon}^*(\mathbf{x}) \rangle_\Omega \rangle_{ens} \quad \text{if} \quad V \to \infty \tag{72}$$

Taking the ensemble average of (17) and accounting for (72), we find that

$$\mathbb{C}^m : \langle \boldsymbol{\epsilon}^*(\mathbf{x}) \rangle_\Omega \simeq (\mathbb{C}^m - \mathbb{C}^i) : [\mathbf{E} + \langle \boldsymbol{\Upsilon} \rangle_{ens} : \mathbb{C}^m : \langle \boldsymbol{\epsilon}^*(\mathbf{x}) \rangle_\Omega] \,, \tag{73}$$

Consequently, the final expression of the effective tensor (21) for random media is slightly modified, $\boldsymbol{\Upsilon}$ now being replaced by its ensemble average $\langle \boldsymbol{\Upsilon} \rangle_{ens}$. In what follows, we shall examine the properties of $\langle \boldsymbol{\Upsilon} \rangle_{ens}$ given by

the expression

$$\langle \boldsymbol{\Upsilon} \rangle_{ens} = \sum_{\boldsymbol{\xi} \neq \mathbf{0}} \langle P(\boldsymbol{\xi}) \rangle_{ens} \boldsymbol{\Gamma}^m(\boldsymbol{\xi}). \tag{74}$$

Considering the integral over the volume of one particle V_p of arbitrary shape located at $\mathbf{x}_c$ and the definition of two functions $\mathcal{F}(\boldsymbol{\xi})$ and $\mathcal{P}(\boldsymbol{\xi})$

$$\int_{V_p} e^{i\boldsymbol{\xi}.\mathbf{x}} d\mathbf{x} = \mathcal{F}(\boldsymbol{\xi}).e^{i\boldsymbol{\xi}.\mathbf{x}_c}, \quad \mathcal{P}(\boldsymbol{\xi}) = \frac{1}{V_p^2} \mathcal{F}(\boldsymbol{\xi}) \mathcal{F}(-\boldsymbol{\xi}) \tag{75}$$

Here, $\mathcal{F}(\boldsymbol{\xi})$ is the integral on the same volume V_p located at the origin. In the scattering theory, $\mathcal{F}(\boldsymbol{\xi})$ and $\mathcal{P}(\boldsymbol{\xi})$ are called form factors and are equivalent to the definitions $I(\boldsymbol{\xi})$ and $P(\boldsymbol{\xi})$ for the case of one particle. For random distribution of particles, $P(\boldsymbol{\xi})$ in (14–74) can be replaced by the ensemble average $\langle P(\boldsymbol{\xi}) \rangle_{ens}$. The latter is linked to the form factor $\mathcal{P}(\boldsymbol{\xi})$, structure factor $S(\boldsymbol{\xi})$, and scattering intensity $\mathcal{I}(\boldsymbol{\xi})$ of the system via the relations

$$\begin{aligned} \langle P(\boldsymbol{\xi}) \rangle_{ens} &= \frac{V_p}{V} \mathcal{I}(\boldsymbol{\xi}), \quad \mathcal{I}(\boldsymbol{\xi}) = \mathcal{P}(\boldsymbol{\xi}) S(\boldsymbol{\xi}), \\ S(\boldsymbol{\xi}) &= \frac{1}{N} \left\langle \sum_i^N e^{i\boldsymbol{\xi}\cdot\mathbf{x}_i} \sum_i^N e^{-i\boldsymbol{\xi}\cdot\mathbf{x}_i} \right\rangle_{ens}. \end{aligned} \tag{76}$$

In (76), we assume that there are N particles of characteristic dimension R in a cubic cell of dimension a and $\mathbf{x}_i$ is the location of the particle number i in the cell. It is interesting to note that $\mathcal{I}(\boldsymbol{\xi})$ can be obtained experimentally by scattering techniques. Conversely, theoretical results of $\mathcal{I}(\boldsymbol{\xi})$ for some ideal systems are known, for example, those governed by Ornstein–Zernike (OZ) equation and Percus–Yevick (PY) closure approximation. As long as $\mathcal{I}(\boldsymbol{\xi})$ is known, the infinite lattice sums S_i can also be computed. At the infinite volume limit $R/a \to 0$, taking R as the radius of the sphere having the same

volume as V_p (i.e., $V_p = 4\pi R^3/3$), those sums can be replaced by the integrals

$$S_i = \frac{1}{6\pi^2}\int \bar{\eta}_i^2 \mathcal{I}(\boldsymbol{\xi}) d\boldsymbol{\eta}, \quad S_{i+3} = \frac{1}{6\pi^2}\int \bar{\eta}_i^4 \mathcal{I}(\boldsymbol{\xi}) d\boldsymbol{\eta},$$
$$S_{i+6} = \frac{1}{6\pi^2}\int \bar{\eta}_j^2 \bar{\eta}_k^2 \mathcal{I}(\boldsymbol{\xi}) d\boldsymbol{\eta}, \quad \boldsymbol{\eta} = R\boldsymbol{\xi},$$
$$i, j, k = 1, 2, 3, \quad i \neq j \neq k \neq i. \tag{77}$$

In the case where the particles are identical spheres of radius R with isotropic distribution (see Fig. 5a), the associated isotropic quantities (*iso* as superscript) $\mathcal{I}^{iso}(\xi)$, $\mathcal{P}^{iso}(\xi)$, and $S^{iso}(\xi)$ are all functions of the modulus ξ (or η). In addition, the structure factor $S^{iso}(\xi)$ is related to the radial distribution function $g(r)$ via the relation

$$S^{iso}(\xi) = 1 + 3f\int_0^\infty \frac{\sin\eta\bar{r}}{\eta}[g(r) - 1]\bar{r}d\bar{r}, \quad \bar{r} = \frac{r}{R}, \tag{78}$$

For nonoverlapping spheres $g(r) = 0$ when $\bar{r} < 2$, the following property holds:

$$\int_0^\infty \frac{[\eta\cos\eta - \sin\eta]^2}{\eta^5}\sin(\eta\bar{r})d\eta = 0, \quad \forall\bar{r} \geq 2. \tag{79}$$

As a result, the integrals S_i admit the simple expressions

$$S_1 = S_2 = S_3 = \frac{(1-f)}{3}, \quad S_4 = S_5 = S_6 = \frac{(1-f)}{5},$$
$$S_7 = S_8 = S_9 = \frac{(1-f)}{15}. \tag{80}$$

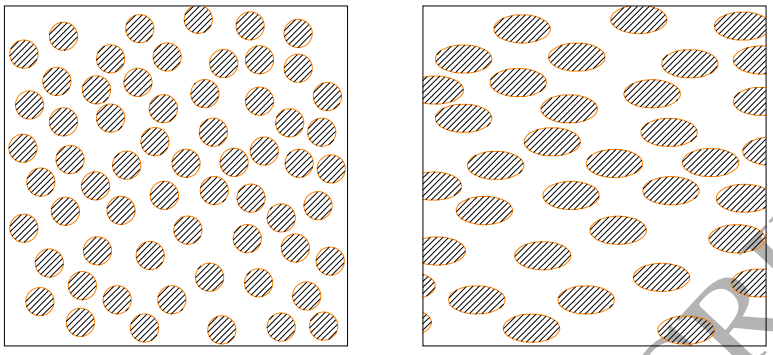

Figure 5: Randomly distributed spheres (left) and ellipsoids (right). The distribution of spheres of radius R is isotropic. The latter is obtained by scaling the former with ratios $1/\chi_1$, $1/\chi_2$, and $1/\chi_3$ along directions $1, 2$, and 3.

Substituting (80) back into (50, 51, 52), we obtain:

$$\kappa^e = \kappa_m - \frac{f}{\frac{1}{\kappa_m-\kappa_i} - \frac{3(1-f)}{3\kappa_m+4\mu_m}},$$
$$\mu^e = \mu^{e*} = \mu_m - \frac{f}{\frac{1}{\mu_m-\mu_i} - \frac{6(\kappa_m+2\mu_m)(1-f)}{5\mu_m(3\kappa_m+4\mu_m)}}, \tag{81}$$

Equations (81) show that, at the infinite volume limit, the effective material is isotropic and that its effective elasticity tensor corresponds to the Hashin–Shtrikman bound (Hashin and Shtrikman, 1963), or equivalently to the Mori–Tanaka estimation for spherical inclusions (Mori and Tanaka, 1973). Interestingly, this equivalence has been noted previously in the issue of heat conduction (To et al., 2013) and has recently been rediscovered in linear elasticity.

It is worth noting that the Mori–Tanaka estimate has been recovered along the previous lines using statistical information, including the ergodic hypothesis, although this estimate is usually presented by using different ad hoc assumptions. Indeed, following Benveniste (1987), such an ad hoc assumption

can be expressed as "if introducing a single inclusion into a homogeneous matrix under boundary conditions corresponding to an overall strain $\boldsymbol{\epsilon}_0$ results in an average strain in the inclusion given by $\boldsymbol{\epsilon}_I = \mathbf{T}.\boldsymbol{\epsilon}_0$, then introducing a single inclusion into a deformed matrix having an average strain $\boldsymbol{\epsilon}_M$ will result in an average strain in the inclusion given by $\boldsymbol{\epsilon}_I = \mathbf{T}.\boldsymbol{\epsilon}_M$."

Our results can be compared with full results on random distributions of particles. For example, Segurado and Llorca (2002) modeled the behaviour of composites containing randomly distributed spherical inclusions using finite elements. For low concentrations of inclusions, their results are very close to the Mori–Tanaka estimates, as predicted previously by our developments. However, for higher concentrations where the inclusions strongly interact, the present approach is not sufficiently accurate. In this case, higher-order correlation functions can be used to address these issues, as done by Nguyen et al. (2016) for the heat conduction phenomenon.

For anisotropic distributions of identical ellipsoids, there exists an analytical solution for the special case where the distribution of inclusions can be obtained from an isotropic distribution by uniform dilatation transformation with coefficients $1/\chi_1$, $1/\chi_2$, and $1/\chi_3$ along the three directions $1, 2$, and 3 (see Fig. 5b). In other words, not only are the spherical inclusions transformed into ellipsoids of dimensions R/χ_1, R/χ_2, and R/χ_3 but their coordinates are scaled with the same ratios as well. In doing so, we also obtain a system containing nonoverlapping ellipsoids with the same volume fraction f. To respect the definition of the characteristic length R defined in the beginning of the present subsection, $\chi_1\chi_2\chi_3 = 1$ is assumed. The anisotropic (*ani* as superscript) and isotropic statistical quantities associated to two systems

are interconnected, say

$$\begin{aligned}
\mathcal{P}^{ani}(\boldsymbol{\xi}) &= \mathcal{P}^{iso}\left(\sqrt{\xi_1^2/\chi_1^2+\xi_2^2/\chi_2^2+\xi_3^2/\chi_3^2}\right),\\
S^{ani}(\boldsymbol{\xi}) &= S^{iso}\left(\sqrt{\xi_1^2/\chi_1^2+\xi_2^2/\chi_2^2+\xi_3^2/\chi_3^2}\right),\\
\mathcal{I}^{ani}(\boldsymbol{\xi}) &= \mathcal{I}^{iso}\left(\sqrt{\xi_1^2/\chi_1^2+\xi_2^2/\chi_2^2+\xi_3^2/\chi_3^2}\right).
\end{aligned} \tag{82}$$

Again, by changing the variable, we obtain

$$\begin{aligned}
S_i &= \frac{T_i}{6\pi^2}\int_0^\infty \mathcal{I}^{iso}(\xi')d\eta',\\
\xi' &= \sqrt{\xi_1^2/\chi_1^2+\xi_2^2/\chi_2^2+\xi_3^2/\chi_3^2},\quad \eta' = R\xi'.
\end{aligned} \tag{83}$$

Combined with the results for the isotropic case, S_i admits the simple form

$$S_i = \frac{T_i}{4\pi}(1-f), \tag{84}$$

which results again in a closed-form expression of the effective constants.

5. Numerical examples and comparisons

To illustrate the method described previously, we first consider numerical applications in the case of cubic microstructures. The closed-form solutions derived in this work are used to compute the effective properties, and these results will be compared with exact semi-analytical, numerical, and approximate solutions from the literature including

- Numerical results with NIH approximation (Iwakuma and Nemat-Nasser, 1983; Nemat-Nasser et al., 1982)
- CM-type approximation in electrostatics, which was applied to linear elasticity and carefully compared with other types of solutions by Cohen (2004)

- Exact series expansion of elastic polarizabilities and approximation up to third-order correlation (To) (Torquato, 1997, 1998)
- Semi-analytical solution based on periodic singular distribution (SL) (Sangani and Lu, 1987), using an expansion onto a basis of periodic functions and projection onto a basis of spherical harmonics.
- The multipole expansion (ME) method, which can provide accurate solutions by keeping a high number of terms in the series (Kushch, 2013).

As an example, we choose a specific composite with the same Poisson's ratio in both the matrix and inclusions $\nu_i = \nu_m = 0.3$. Next, the dimensionless effective coefficient C^e_{1111}/μ_m is computed at different contrast ratios μ_i/μ_m. The results tabulated in Table 2 show that the closed-form solution, which is based on NIH approximation, agrees very well with CM and ME solutions in the range $\mu_i/\mu_m \leq 100$ and $f \leq 0.5$. At higher contrasts, some discrepancies are observed between the approaches. However, as noted in previous works (Hoang and Bonnet, 2013; Cohen, 2004), both methods (NH and CM) fail in this range. In this case, only the ME solution provides an accurate solution (Kushch, 2013).

Table 1: Ratio of the effective elastic constants C_{1111}/μ_m of a simple cubic array of sphere, $\nu_i = \nu_m = 0.3$. Comparison between the closed-form solution of the present work (PR), Clausius–Mossotti (CM)-type solution from Cohen (2004), and solutions based on multipole expansion (ME) from Kushch (2013).

μ_i/μ_m	$f = 0.1$			$f = 0.3$			$f = 0.5$		
	PR	CM	ME	PR	CM	ME	PR	CM	ME
0	2.794	2.799	2.799	1.852	1.836	1.818	1.137	1.148	1.048
10	4.097	4.101	4.102	5.913	5.880	5.930	8.580	8.645	9.646
100	4.226	4.248	4.248	6.720	6.758	6.887	10.94	11.453	17.71

The first extreme case is related to void inclusions. By making $\mu_i/\mu_m \to 0$,

the limit of (50–51) yields the following simple expressions:

$$\frac{\kappa^e}{\kappa_m} = 1 - \frac{f(1-\nu_m)}{1-\nu_m-(1+\nu_m)S_3}, \tag{85}$$

$$\frac{\mu^e}{\mu_m} = 1 - \frac{f(1-\nu_m)}{2(S_2-(1-\nu_m)S_3)+1-\nu_m}, \tag{86}$$

$$\frac{\mu^{e*}}{\mu_m} = 1 - \frac{f(1-\nu_m)}{1-\nu_m-(1-2\nu_m)S_1-(5-4\nu_m)S_2}. \tag{87}$$

In the other extreme case of rigid inclusions, that is, $\mu_i/\mu_m \to \infty$, the effective properties can be determined as follows:

$$\frac{\kappa^e}{\kappa_m} = 1 + \frac{f(1-\nu_m)}{(1+\nu_m)S_3}, \tag{88}$$

$$\frac{\mu^e}{\mu_m} = 1 + \frac{f(1-\nu_m)}{2((1-\nu_m)S_3-S_2)}, \tag{89}$$

$$\frac{\mu^{e*}}{\mu_m} = 1 + \frac{f(1-\nu_m)}{(1-2\nu_m)S_1+(5-4\nu_m)S_2}. \tag{90}$$

In these examples, the Poisson's ratio of the matrix is fixed at $\nu_m = 0.3$. The resulting effective properties are plotted in Fig. 6 for spherical voids and Fig. 7 for rigid inclusions.

All figures show that the results obtained by our closed-form solution compare well with Cohen's results. For voids, a discrepancy with Sangani and Lu's results is observed, as with Cohen's results. However, in this case, Cohen (2004) expressed doubts with Sangani and Lu's results. For rigid inclusions, our results coincide in the range of concentrations up to 0.5 with Cohen's results. Cohen compared these results with a few semi-analytical or approximate models, which were found to be accurate in this range of concentrations of inclusions.

In the case of orthotropic materials, one considers distributions of ellipsoids

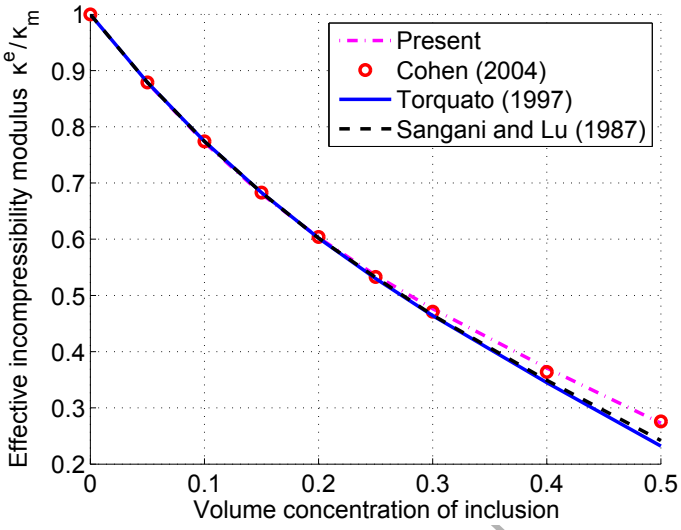

Figure 6: Effective bulk modulus κ^e/κ_m for a simple cubic array of void spheres.

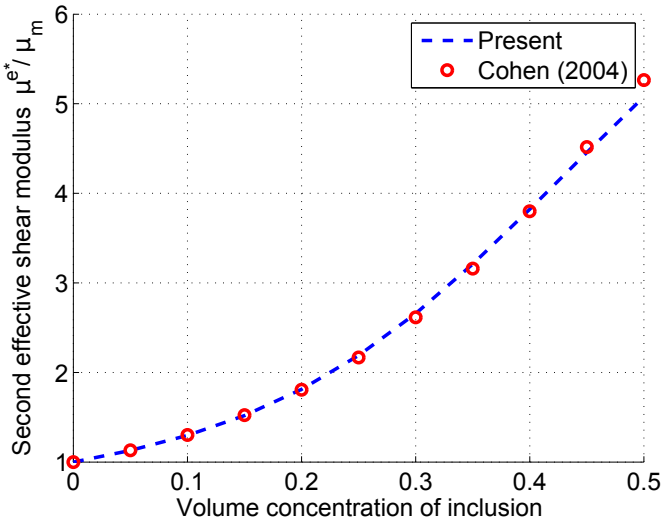

Figure 7: Effective shear modulus μ^{e*}/μ_m for a simple cubic array of rigid spheres.

located at central positions of a cubic lattice. Table 2 shows the comparison between our estimation of $S_i, i = 1..6$ and the results obtained by the computation of the full lattice sums (Iwakuma and Nemat-Nasser, 1983) for

two examples characterized by $\chi_1 = \chi_2$ and the values of $\chi_3/\chi_1 = 4/3$ or $\chi_3/\chi_1 = 2$. This comparison proves that the closed-form expressions obtained in the previous section accurately reproduce the values of S_i computed from the full lattice sum.

Table 2: Comparison between S_i results of the present work (present) and those from Table 3 in Iwakuma and Nemat-Nasser (1983) (IN). The unit cell is cubic of dimension a and the aspect ratio $\chi_1 : \chi_2 : \chi_3$ of the spheroids in SO arrangement are $3 : 3 : 4$ (case 1) and $1 : 1 : 2$ (case 2). Note that results presented by Iwakuma and Nemat-Nasser (1983) are obtained from full lattice sums with resolution $-50 < n_i < 50$.

f		0.05	0.10	0.15	0.20	0.25	0.30	0.35
Case 1								
$S_1 = S_2$	Present	0.268	0.240	0.230	0.216	0.196	0.171	0.148
	IN	0.273	0.255	0.236	0.217	0.196	0.175	0.154
S_3	Present	0.397	0.387	0.376	0.363	0.353	0.345	0.340
	IN	0.392	0.380	0.369	0.359	0.351	0.343	0.337
$S_4 = S_5$	Present	0.172	0.172	0.170	0.164	0.153	0.139	0.123
	IN	0.170	0.171	0.168	0.161	0.152	0.139	0.124
S_6	Present	0.279	0.286	0.292	0.294	0.295	0.297	0.299
	IN	0.275	0.281	0.286	0.290	0.293	0.295	0.297
Case 2								
$S_1 = S_2$	Present	0.218	0.196	0.174	0.148	0.120		
	IN	0.216	0.195	0.172	0.147	0.119		
S_3	Present	0.514	0.505	0.502	0.502	0.508		
	IN	0.507	0.500	0.496	0.497	0.504		
$S_4 = S_5$	Present	0.129	0.126	0.120	0.107	0.088		
	IN	0.127	0.126	0.119	0.107	0.089		
S_6	Present	0.397	0.407	0.422	0.439	0.458		
	IN	0.391	0.403	0.418	0.436	0.455		

Finally, we consider examples concerning orthorhombic and random arrangements of spheroids. For orthorhombic arrangements, the unit cell has the dimensions $a \times a \times 0.5a$ and the spheroids has axes $R \times R \times 0.5R$. Regarding the constitutive materials, the Poisson's ratios of both materials are

$\nu_i = \nu_m = 0.3$ and the Young modulus ratio is $E_i/E_m = 10$. Figures 8 and 9 display the results of analytical solutions for the shear constant obtained in this paper. It is noted that all the curves are relatively close at a small volume fraction ($f \leq 0.15$), which can be explained by the independent behavior of each inclusions. In this range, the dilute estimation is valid, that is, the effective properties only depend on the volume fraction f. At higher f, the interaction of the inclusions is significant and their relative positions in the matrix are not negligible. Although curves start to deviate from each other, the FCO curves are still close to the random curves. This observation suggests that the structure of the FCO arrangements is comparable to the random structures proposed previously.

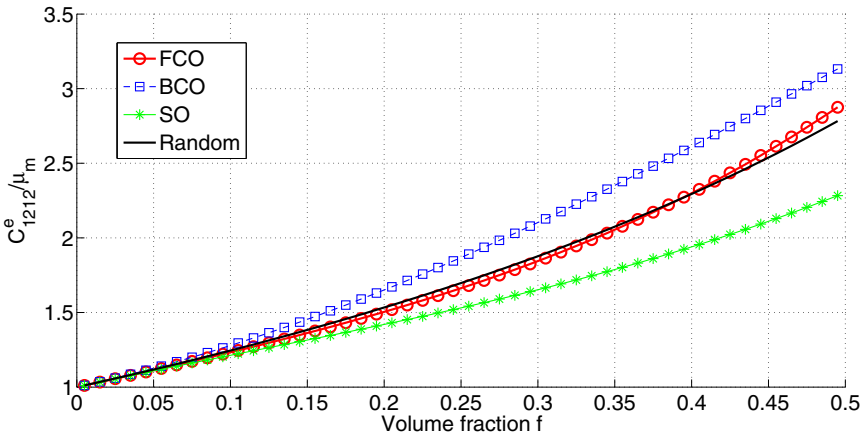

Figure 8: Dimensionless effective shear moduli C^e_{1212}/μ_m for FCO, BCO, SO, and random arrangements of spheroids.

6. Concluding remarks

Effective elasticity tensors of two-phase matrix inclusion composite materials have been obtained when the inclusions are spherical or ellipsoidal and distributed either along the sites of an orthorhombic crystal system or randomly. The basis of the analysis is the eigenstrain integral equation and the

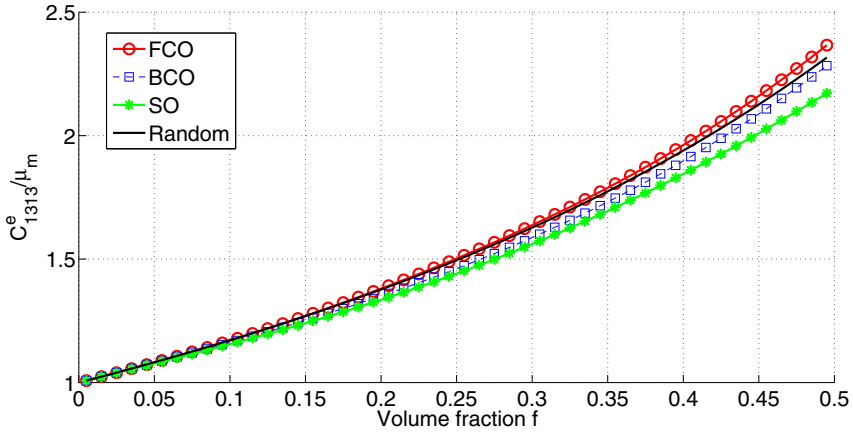

Figure 9: Dimensionless effective shear moduli C^e_{1313}/μ_m for FCO, BCO, SO, and random arrangements of spheroids.

NIH-type estimation (Nemat-Nasser et al., 1982). We have shown that this estimation is related to the use of the "periodic Eshelby tensor" which allows to recover the mean strain within the inclusions when a constant eigenstrain is applied over the periodic set of inclusions.

A first validation is provided in the specific case of cubic materials: all our results fully reproduce those of Cohen (2004), which were obtained by a perturbation method, in relation to the CM approximation of electrostatics. We have shown that the expressions of the components of the elasticity tensor reproduce those of Cohen (2004), in the sense that the lattice sums S_i of the NIH approximation can be obtained using the coefficients obtained by Cohen's perturbation method.

We have shown that our method can also estimate the orthotropic elasticity tensor in the case of arrangements obtained by parallelelipedic lattice cells of spheres or ellipsoids. All closed-form solutions are fully extended to the case of cells containing spheroids. For the case of fully ellipsoidal inclusions, only

lattice sums S_1, S_2, S_3 can be obtained in a closed form, whereas S_4, S_5, S_6 are provided by simple scalar integrals, which are in any case easier to compute than full lattice sums. Our results compare well with those obtained by the full computation of lattice sums as shown by Iwakuma and Nemat-Nasser (1983).

In the case of a random distribution of spheres, the statistical connection of the effective tensor to the structure factor is shown. A closed-form expression is obtained in the infinite volume limit for an isotropic distribution of spheres, which reproduces the Mori–Tanaka estimate. Although this approximation is usually obtained by "ad hoc" assumptions, our work shows that this estimate can be based on precise statistical information, thus extending a result obtained similarily in the case of conduction through a random distribution of spheres (To et al., 2013).

As a final remark, the present method can also be extended to a more general case where the principal axes of ellipsoids (or spheroids) do not necessarily coincide with the axes x_1, x_2, and x_3 of a rectangular unit cell, as considered in this paper. In such situations, it is sufficient to use the linear transformation $\mathbf{L}$ as discussed in section 2; that is, the grid $\boldsymbol{\eta}'$ is obtained by rotation and dilatation of the grid $\boldsymbol{\eta}$. However, in this case, the effective elasticity tensor is no longer orthotropic, and it leads to a larger number of lattice sums S_i to be computed.

References

Benveniste, Y., 1987. A new approach to the application of Mori-Tanaka's theory in composite materials. Mech. Mater. , 147–157.

Benveniste, Y., Milton, G., 2003. New exact results for the effective electric, elastic, piezoelectric and other properties of composite ellipsoid assemblages. J. Mech. Phys. Solids 51, 1773–1813.

Bohren, C.F., Huffman, D.R., 1998. Absorption and scattering of light by small particles. John Wiley & Sons, New York.

Christensenn, R.M., 1979. Mechanics of composite materials. Wiley, N.Y..

Christensen, R., Lo, K., 1979. Solutions for effective shear properties in three phase sphere and cylinder models. J. Mech. Phys. Solids 27, 315–330.

Cohen, I., 2004. Simple algebraic approximations for the effective elastic moduli of cubic arrays of spheres. J. Mech. Phys. Solids 52, 2167–2183.

Eshelby, J., 1957. The determination of the elastic field of an ellipsoidal inclusion, and related problems. Proc. R. Soc. A 241, 376–396.

Eyre, D.J., Milton, G.W., 1999. A fast numerical scheme for computing the response of composites using grid refinement. Eur. Phys. J. Appl. Phys. 6, 41–47.

Hashin, Z., Shtrikman, S., 1963. A variational approach to the theory of the elastic behaviour of multiphase materials. J. Mech. Phys. Solids 11, 127 – 140.

Hill, R., 1965. A self-consistent mechanics of composite materials. J. Mech. Phys. Solids 13, 213 – 222.

Hoang, D.H., Bonnet, G., 2013. Effective properties of viscoelastic heterogeneous periodic media: An approximate solution accounting for the distribution of heterogeneities. Mech. Mater. 56, 71–83.

Hunter, R.J.,White, L.R., 2001. Foundations of colloid science. Oxford University Press, Oxford.

Iwakuma, T., Nemat-Nasser, S., 1983. Composites with periodic microstructure. Comput. Struct. 16, 13–19.

Kaminski, M., 1999. Boundary element method homogenization of the periodic linear elastic fiber composites. Eng. Anal. Bound. Elem. 23, 815–823.

Kaminski, M., 2005. Multiscale homogenization of n-component composites with semi-elliptical random interface defects. Int. J. Solids Struct. 42, 3571–3590.

Kushch, V., 1997. Microstresses and effective elastic moduli of a solid reinforced by periodically distributed spheroidal particles. Int. J. Solids Struct. 34, 1353–1366.

Kushch, V., 2013. Micromechanics of composites. Multipole expansion approach. Butterworth-Heinemann, New York.

Liu, Y., Nishimura, N., Otani, Y., Takahashi, T., Chen, X., Munakata, H., 2005. A fast boundary element method for the analysis of fiber-reinforced composites based on a rigid-inclusion model. J. Appl. Mech.-Trans. ASME 72, 115–128.

Luciano, R., Barbero, E.J., 1994. Formulas for the stiffness of composites with periodic microstructure. Int. J. Solids Struct. 31, 2933–2944.

Michel, J., Moulinec, H., Suquet, P., 1999. Effective properties of composite materials with periodic microstructure: a computational approach. Comput. Meth. Appl. Mech. Eng. 172, 109–143.

Milton, G.W., 2002. The theory of composites. Cambridge Univ. Press, Cambridge.

Monchiet, V., Bonnet, G., 2012. A polarization-based FFT iterative scheme for computing the effective properties of elastic composites with arbitrary contrast. Int. J. Numer. Meth. Eng. 89, 1419–1436.

Mori, T., Tanaka, K., 1973. Average stress in matrix and average elastic energy of materials with misfitting inclusions. Acta. Metall. Mater. 21, 571–574.

Mura, T., 1987. Micromechanics of defects in solids. Kluwer Academic Publisher, New York.

Nemat-Nasser, S., Iwakuma, T., Hejazi, M., 1982. On composites with periodic structure. Mech. Mater. 1, 239–267.

Nguyen, M.T., Monchiet, V., Bonnet, G., To, Q.D., 2016. Conductivity estimations of spherical particle suspension based on triplet structure factor. Phys. Rev. E 93, 022105.

Nunan, K., Keller, J., 1984. Effective coefficients of a composite containing spherical inclusions in a periodic array. J. Mech. Phys. Solids 32, 259–280.

Rössler, E., 2009. Solid state theory: an introduction. Springer Verlag, Berlin.

Sanchez-Palencia, E., 1974. Comportements local et macroscopique d'un type de milieux physiques hétérogènes. Int. J. Eng. Sci. 12, 331–351.

Sanchez-Palencia, E., 1980. Non-homogeneous media and vibration theory. Lecture Notes in Physics, Volume 127. Springer Verlag, Berlin.

Sangani, A.S., Lu, W., 1987. Elastic coefficients of composites containing spherical inclusions in a periodic array. J. Mech. Phys. Solids 35, 1–21.

Segurado, J., Llorca, J., 1987. A numerical approximation to the elastic properties of sphere-reinforced composites. J. Mech. Phys. Solids 50, 2107–2121.

To, Q.D., Bonnet, G., 2015. Conductivity of periodic composites made of matrix and polydispersed aggregates. Phys. Rev. E 91, 023206.

To, Q.D., Bonnet, G., To, V.T., 2013. Closed-form solutions for the effective conductivity of two-phase periodic composites with spherical inclusions. Proc. R. Soc. A 469, 1471–2946.

Torquato, S., 1997. Effective stiffness tensor of composite media. I. Exact series expansions. J. Mech. Phys. Solids 45, 1421–1448.

Torquato, S., 1998. Effective stiffness tensor of composite media : II. Applications to isotropic dispersions. J. Mech. Phys. Solids 46, 1411 – 1440.

Torquato, S., 2001. Random heterogeneous materials: microstructure and macroscopic properties. Springer Verlag, Berlin.

Tsukrov, I. , Kachanov, M., 2000. Effective moduli of an anisotropic material with elliptical holes of arbitrary orientational distribution. Int. J. Solids Struct. 37, 3571–3590.

Appendix A. Algebraic operations between cubic tensors

Algebraic operations between cubic tensors can be made simple using the base $\mathcal{B} = \{\mathbb{I}, \mathbf{i} \otimes \mathbf{i}, \mathbb{N}\}$ and Table A.3 where $\mathbb{I}$ is the fourth-order identity tensor and $\mathbf{i}$ the second-order identity tensor. Tensor $\mathbb{N}$ in this case is equal to

$$\mathbb{N} = \mathbf{e}_1 \otimes \mathbf{e}_1 \otimes \mathbf{e}_1 \otimes \mathbf{e}_1 + \mathbf{e}_2 \otimes \mathbf{e}_2 \otimes \mathbf{e}_2 \otimes \mathbf{e}_2 + \mathbf{e}_3 \otimes \mathbf{e}_3 \otimes \mathbf{e}_3 \otimes \mathbf{e}_3, \tag{A.1}$$

in which $\mathbf{e}_1, \mathbf{e}_2$, and $\mathbf{e}_3$ are the unit vectors along directions $1, 2$, and 3 of the coordinate system. The inversion of cubic tensors is also simple enough to work with symbolic notations, for example,

$$[\lambda \mathbf{i} \otimes \mathbf{i} + 2\mu\mathbb{I} + \alpha\mathbb{N}]^{-1} = -\frac{\lambda}{(2\mu+\alpha)(3\lambda+2\mu+\alpha)}\mathbf{i} \otimes \mathbf{i} + \frac{1}{2\mu}\mathbb{I} - \\ -\frac{\alpha}{2\mu(2\mu+\alpha)}\mathbb{N} \tag{A.2}$$

Table A.3: Basic algebraic operations between tensors in base $\mathcal{B}$

:	$\mathbb{I}$	$\mathbf{i}\otimes\mathbf{i}$	$\mathbb{N}$
$\mathbb{I}$	$\mathbb{I}$	$\mathbf{i}\otimes\mathbf{i}$	$\mathbb{N}$
$\mathbf{i}\otimes\mathbf{i}$	$\mathbf{i}\otimes\mathbf{i}$	$3\mathbf{i}\otimes\mathbf{i}$	$\mathbf{i}\otimes\mathbf{i}$
$\mathbb{N}$	$\mathbb{N}$	$\mathbf{i}\otimes\mathbf{i}$	$\mathbb{N}$

Thus, when combined with (10), the tensor $\boldsymbol{\Upsilon}$ can be rewritten in base $\mathcal{B}$ as

$$\boldsymbol{\Upsilon} = A\mathbb{I} + B\mathbf{i}\otimes\mathbf{i} + C\mathbb{N} \tag{A.3}$$

where the coefficients A, B, C are defined by the formulae:

$$\begin{aligned} A &= -\frac{2\left(\lambda_m+\mu_m\right)}{\mu_m\left(\lambda_m+2\mu_m\right)}S_7 + \frac{1}{\mu_m}S_1, \\ B &= -\frac{\left(\lambda_m+\mu_m\right)}{\mu_m\left(\lambda_m+2\mu_m\right)}S_7, \\ C &= -\frac{\left(\lambda_m+\mu_m\right)}{\mu_m\left(\lambda_m+2\mu_m\right)}S_4 + \frac{3\left(\lambda_m+\mu_m\right)}{\mu_m\left(\lambda_m+2\mu_m\right)}S_7. \end{aligned} \tag{A.4}$$

Only three lattice sums appear, due to the cubic symmetry (49). In addition, due to (29), these sums are interdependent via the relation $S_4 + 2S_7 = S_1$. As each phase is an isotropic material, the tensors $\mathbb{C}^m$ and $(\mathbb{C}^i - \mathbb{C}^m)^{-1}$, etc. in (21) can be expressed in base $\mathcal{B}$. This evidence leads to the final cubic effective tensor $\mathbb{C}^e$

$$\mathbb{C}^e = \lambda^e\mathbf{i}\otimes\mathbf{i} + 2\mu^e\mathbb{I} + \alpha^e\mathbb{N} \tag{A.5}$$

where the coefficients λ^e, μ^e, and α^e can be used to determine the three effective elasticity coefficients κ^e, μ^{e*} by

$$\kappa^e = \frac{3\lambda^e + 2\mu^e + \alpha^e}{3}, \quad \mu^{e*} = \frac{2\mu^e + \alpha^e}{2} \tag{A.6}$$

The final explicit expressions of κ^e, μ^e, and μ^{e*} are given in (50) and (51).

Appendix B. Computation of T_i coefficients for spheroidal inclusions

In the spherical coordinate system (r, θ, ϕ), the surface integrals have the following forms:

$$
\begin{aligned}
&T_1 = T_2 = \int \frac{\sin^2\phi \sin^2\theta \sin\theta d\theta d\phi}{\sin^2\theta + \chi^2\cos^2\theta}, \quad T_3 = \int \frac{\chi^2\cos^2\theta \sin\theta d\theta d\phi}{\sin^2\theta + \chi^2\cos^2\theta},\\
&T_4 = T_5 = \int \frac{\sin^4\phi \sin^4\theta \sin\theta d\theta d\phi}{[\sin^2\theta + \chi^2\cos^2\theta]^2}, \quad T_6 = \int \frac{\chi^4\cos^4\theta \sin\theta d\theta d\phi}{[\sin^2\theta + \chi^2\cos^2\theta]^2},\\
&T_7 = T_8 = \int \frac{\chi^2\cos^2\theta \sin^2\theta \sin^2\phi \sin\theta d\theta d\phi}{[\sin^2\theta + \chi^2\cos^2\theta]^2},\\
&T_9 = \int \frac{\sin^4\theta \sin^2\phi \cos^2\phi \sin\theta d\theta d\phi}{[\sin^2\theta + \chi^2\cos^2\theta]^2}; \quad \theta \in [0, \pi], \quad \phi \in [0, 2\pi]. \quad \text{(B.1)}
\end{aligned}
$$

Eliminating ϕ and making variable change $t = \cos\theta$, the integrals T_i can be reduced to more tractable forms:

$$
\begin{aligned}
&T_1 = T_2 = \pi \int_{-1}^{1} \frac{(1-t^2)dt}{(1-t^2) + \chi^2 t^2}, \quad T_3 = 2\pi \int_{-1}^{1} \frac{\chi^2 t^2 dt}{(1-t^2) + \chi^2 t^2},\\
&T_4 = T_5 = \frac{3\pi}{4} \int_{-1}^{1} \frac{(1-t^2)^2 dt}{[(1-t^2) + \chi^2 t^2]^2}, \quad T_6 = 2\pi \int_{-1}^{1} \frac{\chi^4 t^4 dt}{[(1-t^2) + \chi^2 t^2]^2},\\
&T_7 = T_8 = \pi \int_{-1}^{1} \frac{\chi^2(1-t^2) t^2 dt}{[(1-t^2) + \chi^2 t^2]^2}, \quad T_9 = \frac{\pi}{4} \int_{-1}^{1} \frac{(1-t^2)^2 dt}{[(1-t^2) + \chi^2 t^2]^2}.
\end{aligned} \quad \text{(B.2)}
$$

Finally, the integration leads to the closed-form expressions given in (71).

Appendix C. Computation of tensors $T_i, i = 4..6$ for fully ellipsoidal inclusions

For fully ellipsoidal inclusions, coefficients $T_i, i = 4..6$ are given by the scalar integrals

$$T_i = 4\frac{\chi_i^4}{\chi_3^4}\int_0^{\pi/2} F_i(\phi)d\phi \tag{C.1}$$

where F_i are the following functions:

$$\begin{aligned} F_4 &= \frac{M(1-4\zeta)+\zeta(2\zeta+1)Q}{\zeta^4 Q^5} cos^4(\phi) \\ F_5 &= \tan^4\phi F_4 \\ F_6 &= \frac{P\zeta(\zeta+2)-3\zeta M}{\zeta^3 Q^5} \end{aligned} \tag{C.2}$$

where $\zeta = \frac{\cos^2\phi\chi_1^2+\sin^2\phi\chi_2^2}{\chi_3^2}$,

$$Q = \sqrt{\frac{\zeta-1}{\zeta}} \tag{C.3}$$

$$M = \tanh^{-1}(Q) \tag{C.4}$$

for $\zeta > 1$,

$$Q = \sqrt{\frac{1-\zeta}{\zeta}} \tag{C.5}$$

$$M = \arctan(Q) \tag{C.6}$$

for $\zeta < 1$, whereas

$$F_4 = \frac{16}{5}\cos^4(\phi) \tag{C.7}$$

$$\begin{aligned} F_5 &= \tan^4\phi F_4 \\ F_6 &= \frac{2}{5} \end{aligned} \tag{C.8}$$

for $\zeta = 1$.